

## Cosmological Preference for a Positive Neutrino Mass at $2.7\sigma$ : A Joint Analysis of DESI DR2, DESY5, and DESY1 Data

GUO-HONG DU ,<sup>1</sup> TIAN-NUO LI ,<sup>1</sup> PENG-JU WU ,<sup>2</sup> JING-FEI ZHANG ,<sup>1</sup> AND XIN ZHANG ,<sup>1,3,4</sup>

<sup>1</sup>Key Laboratory of Cosmology and Astrophysics (Liaoning Province), College of Sciences, Northeastern University, Shenyang 110819, China

<sup>2</sup>School of Physics, Ningxia University, Yinchuan 750021, China

<sup>3</sup>MOE Key Laboratory of Data Analytics and Optimization for Smart Industry, Northeastern University, Shenyang 110819, China

<sup>4</sup>National Frontiers Science Center for Industrial Intelligence and Systems Optimization, Northeastern University, Shenyang 110819, China

### ABSTRACT

Neutrinos and dark energy (DE) have entered a new era of investigation, as the latest DESI baryon acoustic oscillation measurements tighten the constraints on the neutrino mass and suggest that DE may be dynamical rather than a cosmological constant. In this work, we investigate the cosmological implications of simultaneously incorporating  $\sum m_\nu$  and  $N_{\text{eff}}$  within the framework of dynamical DE. A joint analysis of DESI DR2, cosmic microwave background, DESY5 supernova, and DESY1 weak lensing data yields a total neutrino mass of  $\sum m_\nu = 0.098^{+0.016}_{-0.037}$  eV, indicating a preference for a positive neutrino mass at the  $2.7\sigma$  level within the  $w_0w_a$ CDM framework. This work highlights the important influence of the strength of evidence for dynamically evolving DE on the measurement of neutrino mass, with stronger evidence for DE dynamics leading to a larger neutrino mass. These results underscore the importance of measuring the neutrino mass within the framework of dynamical DE, particularly in light of the forthcoming, more complete DESI data releases.

*Keywords:* Cosmology (343) — Cosmological neutrinos (338) — Neutrino masses (1102) — Dark energy (351)

### 1. INTRODUCTION

Over the past two decades, the accelerated expansion of the late-time universe has been confirmed by a variety of cosmological observations, such as Type Ia supernova (SN) (Riess et al. 1998; Perlmutter et al. 1999), cosmic microwave background (CMB) (Aghanim et al. 2020a), and baryon acoustic oscillations (BAO) (Alam et al. 2017, 2021), which prompted extensive investigations into the nature of dark energy (DE). The standard  $\Lambda$ CDM model, invoking a cosmological constant  $\Lambda$  and cold dark matter (CDM), is remarkably successful in explaining cosmological observations. However, from a theoretical perspective, the cosmological constant faces the “fine-tuning” and “cosmic coincidence” problems (Sahni & Starobinsky 2000; Bean et al. 2005). Moreover, new observational data pose greater challenges to  $\Lambda$ CDM.

Recently, the Dark Energy Spectroscopic Instrument (DESI) has published its second data release (DR2), incorporating BAO measurements from over 14 million extragalactic sources, based on three years of observations. The DESI

DR2 BAO combined with CMB and SN data, indicates a statistically significant deviation ( $2.8 - 4.2\sigma$ ) from the  $\Lambda$ CDM paradigm, instead favoring a dynamically evolving DE model using the Chevallier–Polarski–Linder (CPL) equation of state (EoS) parameterization,  $w(a) = w_0 + w_a(1-a)$  (Abdul Karim et al. 2025). Interestingly, Giarè et al. (2024) investigated other extended parameterizations using DESI BAO, CMB, and SN data, and their results further reinforce the preference for dynamical DE. These findings provide stronger evidence for dynamically evolving DE and have stimulated numerous efforts to develop and test explanations beyond the  $\Lambda$ CDM framework, such as various DE models (Li et al. 2024; Escamilla et al. 2024; Sabogal et al. 2024; Wang & Piao 2024; Dinda & Maartens 2025; Li et al. 2025d; Huang et al. 2025; Li et al. 2025b; Wu 2025; Li & Zhang 2025; Li & Wang 2025; Barua & Desai 2025; Yashiki 2025; Ling et al. 2025; Goswami & Das 2025; Yang et al. 2025b; Pang et al. 2025; You et al. 2025; Özülker et al. 2025; Cheng et al. 2025a; Pan et al. 2025; Silva & Nunes 2025; Lee et al. 2025) and alternative cosmological scenarios (Roy Choudhury & Okumura 2024; Wu & Zhang 2024; Du et al. 2025b; Jiang et al. 2025; Ye et al. 2025; Du et al. 2025a; Feng et al. 2025; Pan & Ye 2025; Wang & Piao 2025; Cai et al. 2025; Li et al. 2025a; Odintsov et al. 2025; Nojiri et al. 2025; Yang et al. 2025;

Corresponding author: Xin Zhang  
 zhangxin@mail.neu.edu.cn

Kumar et al. 2025; Li et al. 2025e; Roy Choudhury 2025; Li et al. 2025c; Giarè et al. 2025; Liu et al. 2025; Yao & Liu 2025; Cheng et al. 2025b; Bhattacharjee et al. 2025; Afroz & Mukherjee 2025).

In addition to DE, neutrinos also play a significant role in the evolution of the late-time universe. In the standard model of particle physics, neutrinos are considered massless particles. However, measurements of the number density of solar and atmospheric neutrinos indicate oscillatory behavior, which provides evidence for neutrino mass. The results from atmospheric neutrino experiments probing their mass-squared differences indicate  $|\Delta m_{32}^2| \approx 2.4 \times 10^{-3}$  eV<sup>2</sup>, while the measurements from solar neutrinos yield  $\Delta m_{21}^2 \approx 7.4 \times 10^{-5}$  eV<sup>2</sup> (Navas et al. 2024). This configuration implies that at least two neutrino masses must be non-zero, and the lower limits on the total neutrino mass can be estimated:  $\sum m_\nu > 0.06$  eV for the normal hierarchy (NH) scheme, while the inverted hierarchy (IH) requires  $\sum m_\nu > 0.10$  eV (Esteban et al. 2020; de Salas et al. 2021). In addition, direct measurements such as the KATRIN experiment provide competitive upper bounds on the total neutrino mass, currently  $\sum m_\nu < 1.35$  eV (Aker et al. 2025).

The DESI collaboration has recently reported that, when combining the DESI DR2 BAO data with CMB data, the cosmological upper limit on the total neutrino mass is  $\sum m_\nu \lesssim 0.064$  eV at the 95% confidence level in the  $\Lambda$ CDM model (also assuming three degenerate neutrino states). This is alarmingly close to the lower limits established by oscillation experiments for the NH and is in tension with the IH. Furthermore, when the physical prior  $\sum m_\nu > 0$  is relaxed to allowing the unphysical region  $\sum m_\nu < 0$  (employed in the DESI analysis), the cosmological observational data favor a negative neutrino mass, as reported by several independent studies (Naredo-Tuero et al. 2024; Elbers et al. 2025a; Green & Meyers 2025). Interestingly, when considering extended cosmological scenarios, particularly dynamical DE models, the constraint on the neutrino mass is relaxed to  $\sum m_\nu < 0.16$  eV, thereby restoring consistency with oscillation experiments (Abdul Karim et al. 2025). This is due to the strong degeneracy between the EoS of DE and neutrino mass (Hannestad 2005; Zhang 2017; Yang et al. 2017; Roy Choudhury & Choubey 2018), and the DESI results favor the evolution of DE EoS crossing from  $w < -1$  at early times to  $w > -1$  at late times, which leads to a larger neutrino mass (Zhang 2016). Moreover, the inferred Hubble constant of DESI DR2 is even lower than the  $\Lambda$ CDM value of  $67.4 \text{ km s}^{-1} \text{ Mpc}^{-1}$ ,

thereby exacerbating the Hubble tension<sup>1</sup>. It is well known that the Hubble constant  $H_0$  and the effective number of relativistic species  $N_{\text{eff}}$ , a key parameter in neutrino physics, are positively correlated (see, e.g., Gariazzo et al. 2014; Leistedt et al. 2014; Zhang et al. 2015; Feng et al. 2017; Pan et al. 2024; Escudero & Abazajian 2025). Therefore, within the present context, it is imperative to include the influence of  $N_{\text{eff}}$  on the measurement of neutrino mass.

In this paper, we examine the cosmological implications of simultaneously incorporating  $\sum m_\nu$  and  $N_{\text{eff}}$  within the dynamical DE framework. We demonstrate that the joint analysis of the latest cosmological datasets yields a preference for a positive neutrino mass at the  $2.7\sigma$  level, and that the evidence strength for dynamical DE significantly influences the detectability of the neutrino mass.

This work is organized as follows. In Section 2, we briefly introduce the models considered in this work, along with the cosmological data utilized in the analysis. In Section 3, we report the constraint results and make some relevant discussions. The conclusion is given in Section 4.

## 2. METHODOLOGY AND DATA

### 2.1. Models

In cosmology, the total energy density of massive neutrinos is given by (Komatsu et al. 2011)

$$\rho_\nu(a) = \frac{a^{-4}}{\pi^2} \int \frac{q^2 dq}{e^{q/T_{\nu 0}} + 1} \sum_i \sqrt{q^2 + m_i^2 a^2}, \quad (1)$$

where  $q$  is the comoving momentum,  $T_{\nu 0} = (4/11)^{1/3} T_{\text{cmb}} = 1.945$  K and  $T_{\text{cmb}} = 2.725$  K represent the present neutrino and CMB temperature, respectively.  $m_i$  ( $i = 1, 2, 3$ ) are the mass of each neutrino species.

In the early universe, neutrinos were relativistic, thereby  $\rho_\nu$  is proportional to the photon energy density ( $\rho_\gamma$ ), given by (Komatsu et al. 2011)

$$\rho_\nu(a) \rightarrow N_{\text{eff}} \frac{7}{8} \left( \frac{4}{11} \right)^{4/3} \rho_\gamma(a), \quad (2)$$

where  $N_{\text{eff}}$  is the effective number of relativistic neutrino species and in the Standard Model,  $N_{\text{eff}} = 3.044$  (Akita & Yamaguchi 2020; Froustey et al. 2020; Bennett et al. 2021). Equation (1) can therefore be rewritten as

$$\rho_\nu(a) = N_{\text{eff}} \frac{7}{8} \left( \frac{4}{11} \right)^{4/3} \rho_\gamma(a) \sum_i g \left( \frac{m_i}{T_{\nu 0}} a \right), \quad (3)$$

<sup>1</sup> The Hubble tension, a discrepancy exceeding  $5\sigma$  between the CMB estimate of the Hubble constant (assuming a  $\Lambda$ CDM cosmology) (Aghanim et al. 2020a) and the SH0ES (Supernovae and  $H_0$  for the EoS of DE) measurement (Riess et al. 2022), has been extensively discussed in recent years (Bernal et al. 2016; Guo et al. 2019; Vagnozzi 2020; Di Valentino et al. 2020; Cai et al. 2021; Di Valentino et al. 2021; Gao et al. 2021; Vagnozzi 2023; Kamionkowski & Riess 2023; Jin et al. 2025).

where

$$g(y) \equiv \frac{40}{7\pi^4} \int_0^\infty \frac{x^2 \sqrt{x^2 + y^2}}{e^x + 1} dx. \quad (4)$$

It can be demonstrated that when  $a \rightarrow \infty$  (i.e., late-time universe), Equation (3) tends asymptotically to

$$\rho_\nu(a) \rightarrow \frac{\sum m_\nu}{93.14 h^2 \text{ eV}} \rho_{\text{crit},0} a^{-3}, \quad (5)$$

where  $h = H_0/(100 \text{ km s}^{-1} \text{ Mpc}^{-1})$  is the dimensionless Hubble constant.  $\rho_{\text{crit},0} = 3H_0^2/8\pi G$  is the current critical density.

In a flat Friedmann–Robertson–Walker universe, the dimensionless Hubble parameter can be written as

$$E^2(a) \equiv \frac{H^2(a)}{H_0^2} = (\Omega_b + \Omega_c)a^{-3} + \Omega_{\text{de}} f(a) + \Omega_\gamma a^{-4} \left[ 1 + N_{\text{eff}} \frac{7}{8} \left( \frac{4}{11} \right)^{4/3} \sum_i g \left( \frac{m_i}{T_{\nu 0}} a \right) \right], \quad (6)$$

where  $\Omega_\gamma$ ,  $\Omega_b$ ,  $\Omega_c$ , and  $\Omega_{\text{de}}$  represent the current density parameters of photon, baryon, CDM, and DE, respectively, and  $\Omega_\gamma = 2.469 \times 10^{-5}/h^2$  for  $T_{\text{cmb}} = 2.725 \text{ K}$ . Here,  $f(a)$  is the normalized  $a$ -dependent density of DE, given by

$$f(a) = \exp \left( -3 \int_0^{\ln a} [1 + w(a')] d \ln a' \right), \quad (7)$$

where  $w(a)$  is the EoS of DE. In this work, we consider three cosmological models, including the  $\Lambda\text{CDM} + \sum m_\nu + N_{\text{eff}}$  model with  $w = -1$ ,  $w\text{CDM} + \sum m_\nu + N_{\text{eff}}$  model with a constant  $w$ , and  $w_0 w_a \text{CDM} + \sum m_\nu + N_{\text{eff}}$  model, which adopts CPL parameterization form,  $w(a) = w_0 + w_a(1 - a)$  (Chevallier & Polarski 2001; Linder 2003).

## 2.2. Cosmological data

We list the free parameters of these models and the uniform priors applied in Table 1. We compute the theoretical models using the CAMB code (Gelman & Rubin 1992) and use the publicly available sampler Cobaya<sup>2</sup> (Torrado & Lewis 2021) to perform Markov Chain Monte Carlo (MCMC) (Lewis & Bridle 2002; Lewis 2013) analysis. We assess the convergence of the MCMC chains using the Gelman-Rubin statistics quantity  $R - 1 < 0.02$  (Gelman & Rubin 1992) and the MCMC chains are analyzed using the public package GetDist<sup>3</sup> (Lewis 2019). In our main analysis, we consider joint analysis of follow datasets:

<sup>2</sup> <https://github.com/CobayaSampler/cobaya>.

<sup>3</sup> <https://github.com/cmbant/getdist>.

**Table 1.** Flat priors on the main cosmological parameters constrained in this paper.

| Parameter            | Prior                     |
|----------------------|---------------------------|
| $\Omega_b h^2$       | $\mathcal{U}[0.005, 0.1]$ |
| $\Omega_c h^2$       | $\mathcal{U}[0.01, 0.99]$ |
| $\theta_s$           | $\mathcal{U}[0.5, 10]$    |
| $\tau_{\text{reio}}$ | $\mathcal{U}[0.01, 0.8]$  |
| $\log(10^{10} A_s)$  | $\mathcal{U}[1.61, 3.91]$ |
| $n_s$                | $\mathcal{U}[0.8, 1.2]$   |
| $w$ or $w_0$         | $\mathcal{U}[-3, 1]$      |
| $w_a$                | $\mathcal{U}[-3, 2]$      |
| $\sum m_\nu$         | $\mathcal{U}[0, 5]$       |
| $N_{\text{eff}}$     | $\mathcal{U}[1, 6]$       |

- **CMB:** The CMB likelihoods include the Commander likelihood for the TT spectrum and the SimAll likelihood for the EE spectrum (Aghanim et al. 2020a,b), both in the range  $2 \leq \ell \leq 30$ ; the NPIPE high- $\ell$  CamSpec likelihood for the TT spectrum in the range  $30 \leq \ell \leq 2500$ , and for the TE and EE spectra in the range  $30 \leq \ell \leq 2000$  (Efstathiou & Gratton 2019; Rosenberg et al. 2022); as well as the most recent and precise data from the combination of the NPIPE PR4 Planck CMB lensing reconstruction<sup>4</sup> (Carron et al. 2022) and Data Release 6 of the Atacama Cosmology Telescope<sup>5</sup> (Qu et al. 2024).

- **DESI:** The BAO measurements from DESI DR2 include tracers of the bright galaxy sample, luminous red galaxies, emission line galaxies, quasars, and the Lyman- $\alpha$  forest, as summarized in Table IV of Ref. (Abdul Karim et al. 2025).

- **PantheonPlus:** The PantheonPlus comprises 1550 spectroscopically confirmed type Ia supernovae (SNe) from 18 different surveys, covering  $0.01 < z < 2.26$  (Brout et al. 2022)<sup>6</sup>.

- **DESY5:** The DESY5 sample comprises 1635 photometrically classified SNe from the released part of the full 5 yr data of the Dark Energy Survey collaboration (with redshifts in the range  $0.1 < z < 1.3$ ), complemented by 194 low-redshift SNe (with redshifts in the range  $0.025 < z < 0.1$ ), totaling 1829 SNe.<sup>7</sup>

<sup>4</sup> [https://github.com/carronj/planck\\_PR4\\_lensing](https://github.com/carronj/planck_PR4_lensing).

<sup>5</sup> [https://github.com/ACTCollaboration/act\\_dr6\\_lenslike](https://github.com/ACTCollaboration/act_dr6_lenslike).

<sup>6</sup> <https://github.com/PantheonPlusSH0ES/DataRelease>.

<sup>7</sup> <https://github.com/des-science/DES-SN5YR>.

**Table 2.** The  $1\sigma$  confidence regions (or  $2\sigma$  upper limits) of cosmological parameters obtained by the DESI DR2, CMB, DESY5, PantheonPlus, and DESY1 data for the  $\Lambda$ CDM+ $\sum m_\nu + N_{\text{eff}}$ ,  $w$ CDM+ $\sum m_\nu + N_{\text{eff}}$ , and  $w_0 w_a$ CDM+ $\sum m_\nu + N_{\text{eff}}$  models.

| Model/Dataset   | $H_0$                   | $\Omega_m$          | $S_8$               | $w$ or $w_0$               | $w_a$                   | $\sum m_\nu$ [eV]         | $N_{\text{eff}}$       |
|---|-------------------------|---------------------|---------------------|----------------------------|-------------------------|---------------------------|------------------------|
| <b><math>\Lambda</math>CDM + <math>\sum m_\nu + N_{\text{eff}}</math></b> |                         |                     |                     |                            |                         |                           |                        |
| CMB+DESI+DESY5  | $68.37 \pm 0.90$        | $0.3031 \pm 0.0041$ | $0.8215 \pm 0.0083$ | —                          | —                       | < 0.084                   | $3.10 \pm 0.16$        |
| CMB+DESI+DESY5+DESY1  | $68.13 \pm 0.90$        | $0.3016 \pm 0.0040$ | $0.8135 \pm 0.0078$ | —                          | —                       | < 0.085                   | $3.02 \pm 0.16$        |
| <b><math>w</math>CDM + <math>\sum m_\nu + N_{\text{eff}}</math></b>       |                         |                     |                     |                            |                         |                           |                        |
| CMB+DESI+DESY5  | $68.10 \pm 1.00$        | $0.3084 \pm 0.0051$ | $0.8226 \pm 0.0086$ | $-0.956 \pm 0.023$         | —                       | < 0.074                   | $3.24^{+0.18}_{-0.21}$ |
| CMB+DESI+DESY5+DESY1  | $67.78 \pm 0.95$        | $0.3074 \pm 0.0049$ | $0.8152 \pm 0.0077$ | $-0.955 \pm 0.022$         | —                       | < 0.065                   | $3.14 \pm 0.18$        |
| <b><math>w_0 w_a</math>CDM + <math>\sum m_\nu + N_{\text{eff}}</math></b> |                         |                     |                     |                            |                         |                           |                        |
| CMB+DESI+DESY5  | $66.66^{+0.71}_{-0.92}$ | $0.3187 \pm 0.0058$ | $0.8288 \pm 0.0086$ | $-0.753^{+0.054}_{-0.063}$ | $-0.88^{+0.27}_{-0.22}$ | < 0.141                   | $2.85^{+0.40}_{-0.17}$ |
| CMB+DESI+DESY5+DESY1  | $66.54 \pm 0.56$        | $0.3187 \pm 0.0058$ | $0.8199 \pm 0.0081$ | $-0.745^{+0.056}_{-0.063}$ | $-0.91^{+0.26}_{-0.22}$ | $0.098^{+0.016}_{-0.037}$ | $2.46^{+0.60}_{-0.24}$ |
| CMB+DESI+PantheonPlus+DESY1   | $67.37^{+0.77}_{-0.86}$ | $0.3099 \pm 0.0057$ | $0.8182 \pm 0.0084$ | $-0.845 \pm 0.058$         | $-0.58^{+0.24}_{-0.21}$ | < 0.144                   | $2.89^{+0.28}_{-0.18}$ |

**Note.** For the parameter  $\sum m_\nu$ , central values cannot be determined in most cases, and we provide the  $2\sigma$  upper limits. Here,  $H_0$  is in units of  $\text{km s}^{-1} \text{Mpc}^{-1}$ .

- **DESY1:** The DESY1 data, which is based on the analysis of 26 million source galaxies and 6.5 million lens galaxies over a  $1321 \text{ deg}^2$  footprint (Abbott et al. 2018; Baxter et al. 2019), is incorporated into our combined cosmological analysis.

### 3. RESULTS AND DISCUSSIONS

In this section, we present the main parameter constraint results in Table 2 and Figures 1–2. Figure 3 shows the relative variation of the dimensionless Hubble expansion rate.

For the  $\Lambda$ CDM +  $\sum m_\nu + N_{\text{eff}}$  model, we obtain an upper limit on the total neutrino mass of  $\sum m_\nu < 0.084$  eV using CMB+DESI+DESY5 data, and  $\sum m_\nu < 0.085$  eV when DESY1 is included. The inclusion of weak lensing data slightly raises the upper limit on  $\sum m_\nu$ , since the lower clustering amplitude ( $S_8$ ) inferred from weak lensing data allows for larger neutrino masses. Building on this, when a constant DE EoS is introduced, the  $w$ CDM +  $\sum m_\nu + N_{\text{eff}}$  model yields  $\sum m_\nu < 0.065$  eV and  $w = -0.955 \pm 0.022$  using CMB+DESI+DESY5+DESY1 data. This indicates that a constant EoS of DE with  $w > -1$  lowers the neutrino mass upper limit, as illustrated in the left panel of Figure 1, which is in agreement with previous studies (Zhang 2016; Vagnozzi et al. 2018; Du et al. 2025b).

When we further consider a dynamically evolving DE with the CPL parametrization, the CMB+DESI+DESY5+DESY1 data yield  $\sum m_\nu = 0.098^{+0.016}_{-0.037}$  eV, indicating a  $2.7\sigma$  preference of a positive neutrino mass. This positive constraint primarily arises for several reasons. On the one hand, the

detection of a non-zero neutrino mass is strongly influenced by evidence for the dynamical evolution of DE. As shown in Figure 2,  $\sum m_\nu$  is anti-correlated with  $w_a$  and positively correlated with  $w_0$ . The CMB+DESI+DESY5+DESY1 data give  $w_0 = -0.745^{+0.056}_{-0.063}$  and  $w_a = -0.91^{+0.26}_{-0.22}$ , corresponding to evidence for a dynamically evolving DE at the  $\sim 4\sigma$  level, thereby favoring a larger neutrino mass. In contrast, replacing DESY5 with PantheonPlus yields CMB+DESI+PantheonPlus+DESY1 results of  $\sum m_\nu < 0.144$  eV, where the evidence for DE dynamics drops to  $\sim 2\sigma$  ( $w_0 = -0.845 \pm 0.058$ ,  $w_a = -0.58^{+0.24}_{-0.21}$ ), leading only to an upper limit on the neutrino mass. We further test this conclusion by introducing priors with varying strengths on the evidence for dynamically evolving DE; see Appendix A for a detailed discussion. On the other hand,  $\sum m_\nu$  is also anti-correlated with  $S_8$ , and the lower  $S_8$  values preferred by weak lensing data also pushes the neutrino mass higher. Without weak lensing, CMB+DESI+DESY5 only impose an upper limit of  $\sum m_\nu < 0.141$  eV, with a multi-peaked one-dimensional (1D) marginalized posterior distribution, as shown in right panel of Figure 1. The inclusion of DESY1 suppresses the lower-mass peak of the posterior, thereby providing evidence for a positive neutrino mass. Meanwhile, a lower  $H_0$  leads to a reduced  $N_{\text{eff}}$  (though the best-fit value remains close to the standard value of 3.044, the central value falls below 3), which also affects the neutrino mass measurement. Moreover, our result lies below but close to the IH bound and therefore does not support the IH, which is con-

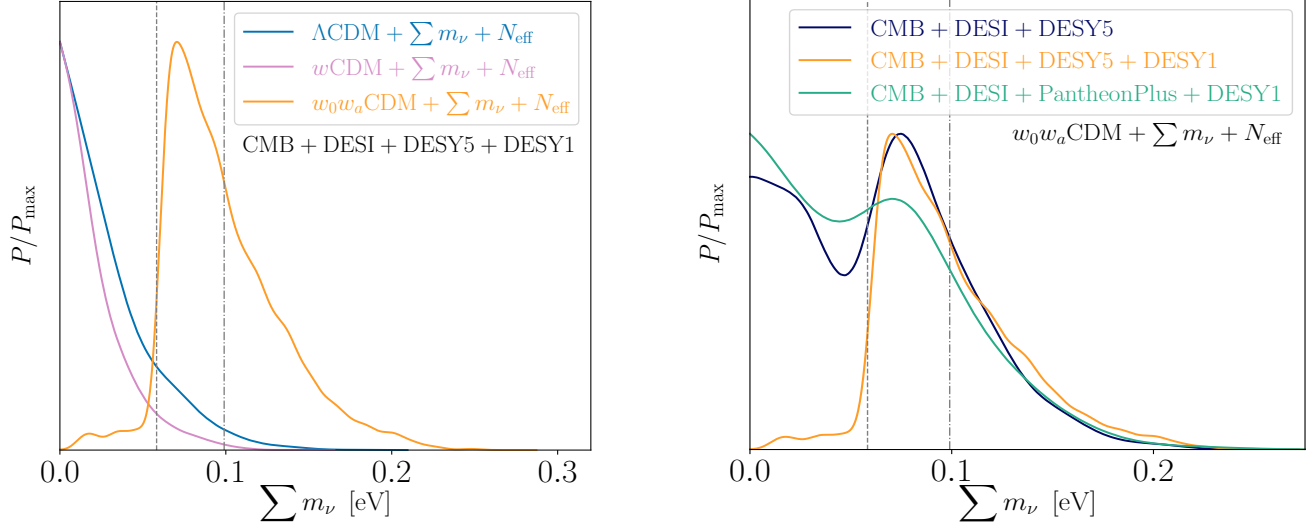


**Figure 1.** The marginalized 1D posterior distributions on  $\sum m_\nu$  using DESI, CMB, DESY5, PantheonPlus, and DESY1 data. The dashed and dash-dotted lines represent the lower bounds of neutrino mass in the NH and IH, respectively. *Left panel:* A comparison of the 1D marginalized posterior distributions for  $\sum m_\nu$  in the  $\Lambda\text{CDM} + \sum m_\nu + N_{\text{eff}}$ ,  $w\text{CDM} + \sum m_\nu + N_{\text{eff}}$ , and  $w_0 w_a \text{CDM} + \sum m_\nu + N_{\text{eff}}$  models using CMB+DESI+DESY5+DESY1 data. *Right panel:* A comparison of the 1D marginalized posterior distributions for  $\sum m_\nu$  in the  $w_0 w_a \text{CDM} + \sum m_\nu + N_{\text{eff}}$  models using CMB+DESI+DESY5, CMB+DESI+DESY5+DESY1, and CMB+DESI+PantheonPlus+DESY1 data.

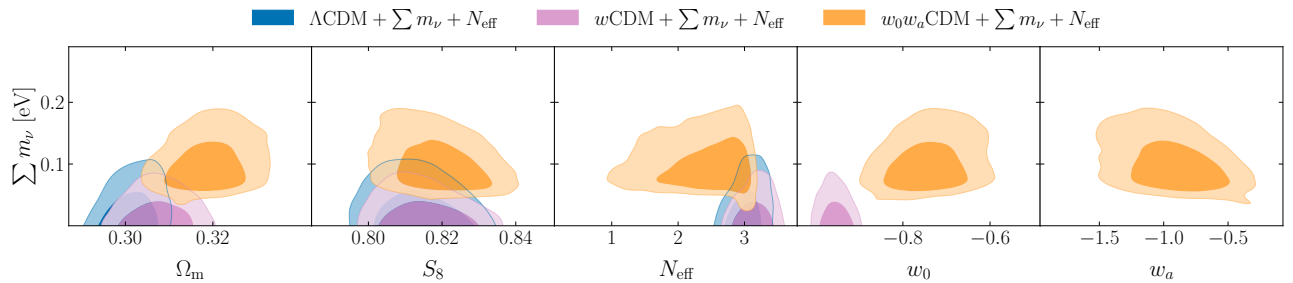


**Figure 2.** A comparison of the two-dimensional marginalized contours between  $\sum m_\nu$  and various other cosmological parameters using CMB+DESI+DESY5+DESY1 data.

sistent with the conclusions of particle physics experiments (De Salas et al. 2018; Gariazzo et al. 2018).

Next, we further illustrate the impact of DE on neutrino mass measurements by examining the evolution of the late-time relative expansion rate. The CMB TT power spectrum data tightly constrain the position and amplitude of the first acoustic peak. The determination of the first peak depends precisely on the angular size of the sound horizon at decoupling,  $\Theta_s \equiv r_s/D_A(z_{\text{LS}})$ , and the redshift of matter–radiation equality,  $z_{\text{eq}}$ . Here, the sound horizon at decoupling  $r_s$  is essentially fixed by the physics of pre-recombination periods, while DE variations are only relevant at late times; therefore,  $r_s$  is unaffected by DE (Vagnozzi et al. 2018). To keep both the angular diameter distance of last scattering  $D_A(z_{\text{LS}})$  and  $z_{\text{eq}}$  approximately fixed, any change in DE must be compensated by shifts in other cosmological

parameters.  $D_A(z_{\text{LS}})$  is given by

$$D_A(z_{\text{LS}}) = \frac{c}{H_0(1+z_{\text{LS}})} \int_0^{z_{\text{LS}}} \frac{1}{E(z)} dz, \quad (8)$$

where  $z_{\text{LS}}$  is the redshift of last scattering. We then define

$$\mathcal{E}(z) = \left. \frac{E(z)_{\Lambda\text{CDM}}}{E(z)_{w\text{CDM}/w_0 w_a \text{CDM}}} \right|_{\Omega_b, \Omega_c, \Omega_{\text{de}}, \sum m_\nu, N_{\text{eff}}} - 1, \quad (9)$$

where the notation  $|_{\Omega_b, \Omega_c, \Omega_{\text{de}}, \sum m_\nu, N_{\text{eff}}}$  indicates that these parameters are held fixed.

The redshift evolution of  $\mathcal{E}(z)$  is shown in Figure 3. It is clear that when the curve lies above zero, DE variations increase the integral in Equation (8), and when it lies below zero, they decrease it. In the  $w\text{CDM}$  model,  $w > -1$  yields a relative expansion rate higher than that in  $\Lambda\text{CDM}$ , resulting in  $\mathcal{E}(z) < 0$  (blue solid line). To keep  $D_A(z_{\text{LS}})$  unchanged, directly reducing  $\Omega_b$ ,  $\Omega_c$ , or  $N_{\text{eff}}$  is undesirable because each shifts  $z_{\text{eq}}$  and would introduce unwanted changes elsewhere

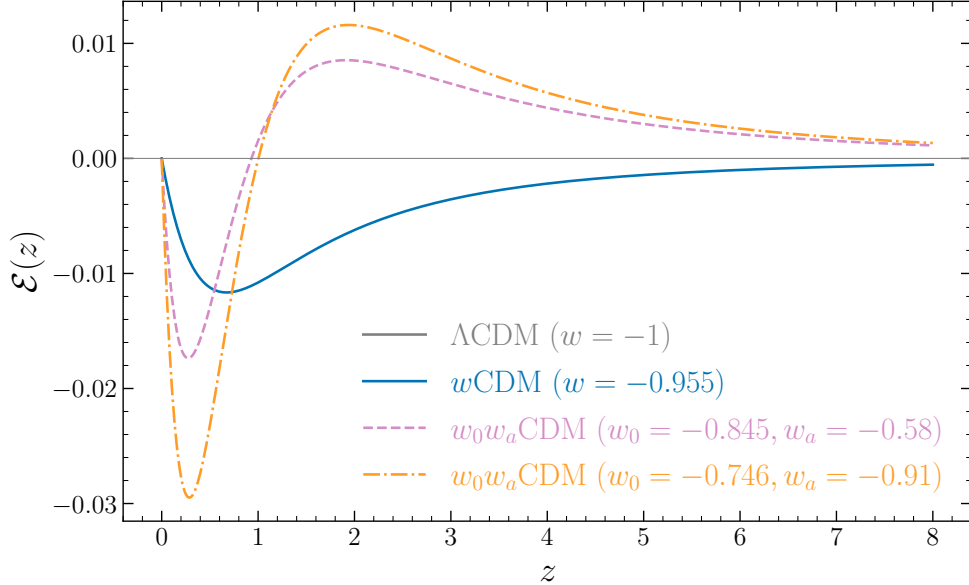


**Figure 3.** The redshift evolution of  $\langle \mathcal{E} \rangle(z)$ . The gray solid curve denotes the  $\Lambda$ CDM model, while the blue solid curve corresponds to the  $w$ CDM model constrained by CMB+DESI+DESY5+DESY1 data ( $w = -0.955$ ). The pink dashed curve represents the  $w_0 w_a$ CDM model using CMB+DESI+PantheonPlus+DESY1 ( $w_0 = -0.845$ ,  $w_a = -0.58$ ). The orange dash-dotted curve is the  $w_0 w_a$ CDM constraints from CMB+DESI+DESY5+DESY1 ( $w_0 = -0.746$ ,  $w_a = -0.91$ ).

in the CMB power spectrum. Instead, lowering  $\sum m_\nu$ , whose effect on  $z_{\text{eq}}$  is minimal, is the most economical option for compensating the reduced integral. Consequently, introducing a constant EoS of DE with  $w > -1$  tightens the upper limit on  $\sum m_\nu$ .

For the  $w_0 w_a$ CDM model, the results exhibit a DE EoS that crosses from  $w < -1$  at early times to  $w > -1$  at late times. Therefore, for  $0 < z \lesssim 1$  the relative expansion rate exceeds that of  $\Lambda$ CDM, whereas for  $z \gtrsim 1$  it falls below it. Since the integral extends to  $z_{\text{LS}} \approx 1090$ , the  $z \gtrsim 1$  region dominates, leading to an overall increase in the integral of Equation 8. This requires a higher  $\sum m_\nu$  to compensate. Moreover, the crossing DE dynamics yield a lower  $H_0$ , which reduces  $N_{\text{eff}}$  and slightly advances  $z_{\text{eq}}$ , which is an effect that coheres with that of increasing  $\sum m_\nu$ . Thus, the  $w_0 w_a$ CDM model yields both a higher  $\sum m_\nu$  and a lower  $N_{\text{eff}}$ , in agreement with DESI results (Adame et al. 2025; Abdul Karim et al. 2025; Elbers et al. 2025b). Finally, as the evidence for dynamically evolving DE strengthens (from the pink dashed line to the orange dash-dot line), the relative expansion rate deviations grow more pronounced, demanding yet larger  $\sum m_\nu$  and smaller  $N_{\text{eff}}$  to offset the DE change, thereby producing stronger evidence for non-zero neutrino mass.

#### 4. CONCLUSION

In this paper, we investigate the cosmological implications of simultaneously including  $\sum m_\nu$  and  $N_{\text{eff}}$  within the framework of dynamical DE. We further clarify the specific impact of dynamical DE on neutrino mass measurements from the

perspectives of parameter degeneracies and the relative expansion rate.

Our joint analysis of DESI DR2, CMB, DESY5, and DESY1 data yields  $\sum m_\nu = 0.098^{+0.016}_{-0.037}$  eV, indicating a preference for a positive neutrino mass at  $2.7\sigma$  level within the  $w_0 w_a$ CDM model when both  $\sum m_\nu$  and  $N_{\text{eff}}$  are simultaneously included, whereas only upper limits are obtained in the  $\Lambda$ CDM and  $w$ CDM frameworks. Moreover, it should be noted that when DESY5 is replaced with PantheonPlus, the evidence for a positive neutrino mass disappears, as the evidence for dynamical DE becomes weaker. The overall outcomes indicate that both the presence of dynamical DE and the strength of its observational evidence have a significant impact on the constraints of the neutrino mass. We test the robustness of our results by investigating how DE affects the detection of neutrino mass and alters the strength of evidence for dynamical DE, through the evolution of the late-time relative expansion rate. We find that as the evidence for dynamical DE strengthens, the deviations in the relative expansion rate become more pronounced, requiring a larger  $\sum m_\nu$  to compensate for the DE changes. This serves as the most economical way to offset the integral variation and consequently enhances the evidence for a non-zero neutrino mass.

Our results indicate that this represents a highly compelling cosmological scenario, and that the DESI dataset has inaugurated a new era for measuring neutrino mass through cosmological observations. With the forthcoming, more complete DESI data releases and the inclusion of full-shape modeling

of the power spectrum, stronger preferences for dynamical DE are likely to emerge, thereby offering promising prospects for further revealing cosmological evidence of a non-zero neutrino mass.

## ACKNOWLEDGMENTS

We thank Sheng-Han Zhou, Jia-Le Ling, and Yi-Min Zhang for their helpful discussions. This work was supported by the National SKA Program of China (Grants Nos. 2022SKA0110200 and 2022SKA0110203), the National Natural Science Foundation of China (Grants Nos. 12473001, 11975072, 11875102, and 11835009), the China Manned Space Program (Grant No. CMS-CSST-2025-A02), and the National 111 Project (Grant No. B16009).

## APPENDIX

### A. IMPACT OF DYNAMICAL DE EVIDENCE ON NEUTRINO MASS

In this Appendix, we report and discuss the impact of the strength of evidence for dynamical DE on neutrino mass constraints. We adopt the constraints on the  $w_0 w_a \text{CDM} + \sum m_\nu + N_{\text{eff}}$  model derived from CMB+DESI+DESY5 data as our baseline. We then impose separately a  $2\sigma$  prior ( $w_0 = -0.86 \pm 0.07$ ,  $w_a = -0.50 \pm 0.25$ ) and a  $5\sigma$  prior ( $w_0 = -0.65 \pm 0.07$ ,  $w_a = -1.25 \pm 0.25$ ). The resulting 1D marginalized posterior distributions of  $\sum m_\nu$  are shown in Figure 4. As expected, for the bimodal structure of the CMB+DESI+DESY5 posterior, the  $2\sigma$  prior suppresses the high-mass peak, yielding an upper limit of  $\sum m_\nu < 0.118$  eV. Conversely, the  $5\sigma$  prior suppresses the low-mass peak, leading to  $\sum m_\nu = 0.083^{+0.046}_{-0.039}$  eV. This further confirms the significant impact of evidence strength for dynamical DE on neutrino mass measurements and ensures the robustness of our conclusions.

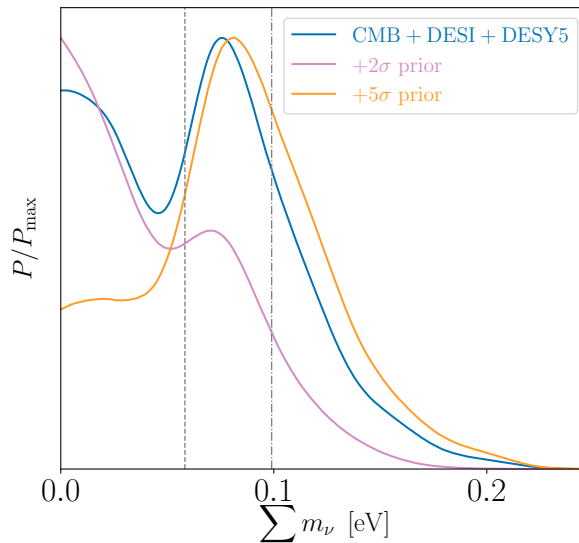


**Figure 4.** The 1D marginalized posterior distributions of  $\sum m_\nu$  in the  $w_0 w_a \text{CDM} + \sum m_\nu + N_{\text{eff}}$  model. The CMB+DESI+DESY5 constraint is regarded as the baseline, shown together with the inclusion of  $2\sigma$  and  $5\sigma$  priors of dynamical DE.

## REFERENCES

- Abbott, T. M. C., et al. 2018, Phys. Rev. D, 98, 043526,  
doi: [10.1103/PhysRevD.98.043526](https://doi.org/10.1103/PhysRevD.98.043526)
- Abdul Karim, M., et al. 2025. <https://arxiv.org/abs/2503.14738>
- Adame, A. G., et al. 2025, JCAP, 02, 021,  
doi: [10.1088/1475-7516/2025/02/021](https://doi.org/10.1088/1475-7516/2025/02/021)
- Afroz, S., & Mukherjee, S. 2025. <https://arxiv.org/abs/2504.16868>
- Aghanim, N., Akrami, Y., Ashdown, M., et al. 2020a, Astron. Astrophys., 641, A6, doi: [10.1051/0004-6361/201833910](https://doi.org/10.1051/0004-6361/201833910)
- Aghanim, N., et al. 2020b, Astron. Astrophys., 641, A5,  
doi: [10.1051/0004-6361/201936386](https://doi.org/10.1051/0004-6361/201936386)
- Aker, M., et al. 2025, Science, 388, adq9592,  
doi: [10.1126/science.adq9592](https://doi.org/10.1126/science.adq9592)

- Akita, K., & Yamaguchi, M. 2020, *J. Cosmol. Astropart. Phys.*, 08, 012, doi: [10.1088/1475-7516/2020/08/012](https://doi.org/10.1088/1475-7516/2020/08/012)
- Alam, S., Ata, M., Bailey, S., et al. 2017, *Mon. Not. Roy. Astron. Soc.*, 470, 2617, doi: [10.1093/mnras/stx721](https://doi.org/10.1093/mnras/stx721)
- Alam, S., Aubert, M., Avila, S., et al. 2021, *Phys. Rev. D*, 103, 083533, doi: [10.1103/PhysRevD.103.083533](https://doi.org/10.1103/PhysRevD.103.083533)
- Barua, S., & Desai, S. 2025, doi: [10.1016/j.dark.2025.101995](https://doi.org/10.1016/j.dark.2025.101995)
- Baxter, E. J., et al. 2019, *Phys. Rev. D*, 99, 023508, doi: [10.1103/PhysRevD.99.023508](https://doi.org/10.1103/PhysRevD.99.023508)
- Bean, R., Carroll, S. M., & Trodden, M. 2005, <https://arxiv.org/abs/astro-ph/0510059>
- Bennett, J. J., Buldgen, G., De Salas, P. F., et al. 2021, *J. Cosmol. Astropart. Phys.*, 04, 073, doi: [10.1088/1475-7516/2021/04/073](https://doi.org/10.1088/1475-7516/2021/04/073)
- Bernal, J. L., Verde, L., & Riess, A. G. 2016, *JCAP*, 10, 019, doi: [10.1088/1475-7516/2016/10/019](https://doi.org/10.1088/1475-7516/2016/10/019)
- Bhattacharjee, S., Halder, S., de Haro, J., Pan, S., & Saridakis, E. N. 2025, <https://arxiv.org/abs/2507.15575>
- Brout, D., et al. 2022, *Astrophys. J.*, 938, 110, doi: [10.3847/1538-4357/ac8e04](https://doi.org/10.3847/1538-4357/ac8e04)
- Cai, R.-G., Guo, Z.-K., Li, L., Wang, S.-J., & Yu, W.-W. 2021, *Phys. Rev. D*, 103, 121302, doi: [10.1103/PhysRevD.103.L121302](https://doi.org/10.1103/PhysRevD.103.L121302)
- Cai, Y., Ren, X., Qiu, T., Li, M., & Zhang, X. 2025, <https://arxiv.org/abs/2505.24732>
- Caron, J., Mirmelstein, M., & Lewis, A. 2022, *JCAP*, 09, 039, doi: [10.1088/1475-7516/2022/09/039](https://doi.org/10.1088/1475-7516/2022/09/039)
- Cheng, H., Di Valentino, E., Escamilla, L. A., Sen, A. A., & Visinelli, L. 2025a, <https://arxiv.org/abs/2505.02932>
- Cheng, H., Yin, Z., Di Valentino, E., Marsh, D. J. E., & Visinelli, L. 2025b, <https://arxiv.org/abs/2506.19096>
- Chevallier, M., & Polarski, D. 2001, *Int. J. Mod. Phys. D*, 10, 213, doi: [10.1142/S0218271801000822](https://doi.org/10.1142/S0218271801000822)
- de Salas, P. F., Forero, D. V., Gariazzo, S., et al. 2021, *JHEP*, 02, 071, doi: [10.1007/JHEP02\(2021\)071](https://doi.org/10.1007/JHEP02(2021)071)
- De Salas, P. F., Gariazzo, S., Mena, O., Ternes, C. A., & Tórtola, M. 2018, *Front. Astron. Space Sci.*, 5, 36, doi: [10.3389/fspas.2018.00036](https://doi.org/10.3389/fspas.2018.00036)
- Di Valentino, E., Melchiorri, A., Mena, O., & Vagnozzi, S. 2020, *Phys. Dark Univ.*, 30, 100666, doi: [10.1016/j.dark.2020.100666](https://doi.org/10.1016/j.dark.2020.100666)
- Di Valentino, E., Mena, O., Pan, S., et al. 2021, *Class. Quant. Grav.*, 38, 153001, doi: [10.1088/1361-6382/ac086d](https://doi.org/10.1088/1361-6382/ac086d)
- Dinda, B. R., & Maartens, R. 2025, *JCAP*, 01, 120, doi: [10.1088/1475-7516/2025/01/120](https://doi.org/10.1088/1475-7516/2025/01/120)
- Du, G.-H., Li, T.-N., Wu, P.-J., et al. 2025a, <https://arxiv.org/abs/2501.10785>
- Du, G.-H., Wu, P.-J., Li, T.-N., & Zhang, X. 2025b, *Eur. Phys. J. C*, 85, 392, doi: [10.1140/epjc/s10052-025-14094-0](https://doi.org/10.1140/epjc/s10052-025-14094-0)
- Efstathiou, G., & Gratton, S. 2019, doi: [10.21105/astro.1910.00483](https://doi.org/10.21105/astro.1910.00483)
- Elbers, W., Frenk, C. S., Jenkins, A., Li, B., & Pascoli, S. 2025a, *Phys. Rev. D*, 111, 063534, doi: [10.1103/PhysRevD.111.063534](https://doi.org/10.1103/PhysRevD.111.063534)
- Elbers, W., et al. 2025b, <https://arxiv.org/abs/2503.14744>
- Escamilla, L. A., Özülker, E., Akarsu, O., Di Valentino, E., & Vázquez, J. A. 2024, <https://arxiv.org/abs/2408.12516>
- Escudero, H. G., & Abazajian, K. N. 2025, *Phys. Rev. D*, 111, 043520, doi: [10.1103/PhysRevD.111.043520](https://doi.org/10.1103/PhysRevD.111.043520)
- Esteban, I., Gonzalez-Garcia, M. C., Maltoni, M., Schwetz, T., & Zhou, A. 2020, *JHEP*, 09, 178, doi: [10.1007/JHEP09\(2020\)178](https://doi.org/10.1007/JHEP09(2020)178)
- Feng, L., Li, T.-N., Du, G.-H., Zhang, J.-F., & Zhang, X. 2025, *Phys. Dark Univ.*, 48, 101935, doi: [10.1016/j.dark.2025.101935](https://doi.org/10.1016/j.dark.2025.101935)
- Feng, L., Zhang, J.-F., & Zhang, X. 2017, *Eur. Phys. J. C*, 77, 418, doi: [10.1140/epjc/s10052-017-4986-3](https://doi.org/10.1140/epjc/s10052-017-4986-3)
- Froustey, J., Pitrou, C., & Volpe, M. C. 2020, *J. Cosmol. Astropart. Phys.*, 12, 015, doi: [10.1088/1475-7516/2020/12/015](https://doi.org/10.1088/1475-7516/2020/12/015)
- Gao, L.-Y., Zhao, Z.-W., Xue, S.-S., & Zhang, X. 2021, *JCAP*, 07, 005, doi: [10.1088/1475-7516/2021/07/005](https://doi.org/10.1088/1475-7516/2021/07/005)
- Gariazzo, S., Archidiacono, M., de Salas, P. F., et al. 2018, *JCAP*, 03, 011, doi: [10.1088/1475-7516/2018/03/011](https://doi.org/10.1088/1475-7516/2018/03/011)
- Gariazzo, S., Giunti, C., & Laveder, M. 2014, <https://arxiv.org/abs/1404.6160>
- Gelman, A., & Rubin, D. B. 1992, *Statist. Sci.*, 7, 457, doi: [10.1214/ss/1177011136](https://doi.org/10.1214/ss/1177011136)
- Giarè, W., Mena, O., Specogna, E., & Di Valentino, E. 2025, <https://arxiv.org/abs/2507.01848>
- Giarè, W., Najafi, M., Pan, S., Di Valentino, E., & Firouzjaee, J. T. 2024, *JCAP*, 10, 035, doi: [10.1088/1475-7516/2024/10/035](https://doi.org/10.1088/1475-7516/2024/10/035)
- Goswami, S., & Das, S. 2025, *Phys. Dark Univ.*, 48, 101951, doi: [10.1016/j.dark.2025.101951](https://doi.org/10.1016/j.dark.2025.101951)
- Green, D., & Meyers, J. 2025, *Phys. Rev. D*, 111, 083507, doi: [10.1103/PhysRevD.111.083507](https://doi.org/10.1103/PhysRevD.111.083507)
- Guo, R.-Y., Zhang, J.-F., & Zhang, X. 2019, *JCAP*, 02, 054, doi: [10.1088/1475-7516/2019/02/054](https://doi.org/10.1088/1475-7516/2019/02/054)
- Hannestad, S. 2005, *Phys. Rev. Lett.*, 95, 221301, doi: [10.1103/PhysRevLett.95.221301](https://doi.org/10.1103/PhysRevLett.95.221301)
- Huang, L., Cai, R.-G., & Wang, S.-J. 2025, <https://arxiv.org/abs/2502.04212>
- Jiang, J.-Q., Giarè, W., Gariazzo, S., et al. 2025, *JCAP*, 01, 153, doi: [10.1088/1475-7516/2025/01/153](https://doi.org/10.1088/1475-7516/2025/01/153)
- Jin, S.-J., Song, J.-Y., Sun, T.-Y., et al. 2025, <https://arxiv.org/abs/2507.12965>
- Kamionkowski, M., & Riess, A. G. 2023, *Ann. Rev. Nucl. Part. Sci.*, 73, 153, doi: [10.1146/annurev-nucl-111422-024107](https://doi.org/10.1146/annurev-nucl-111422-024107)
- Komatsu, E., et al. 2011, *Astrophys. J. Suppl.*, 192, 18, doi: [10.1088/0067-0049/192/2/18](https://doi.org/10.1088/0067-0049/192/2/18)
- Kumar, U., Ajith, A., & Verma, A. 2025, <https://arxiv.org/abs/2504.14419>
- Lee, D. H., Yang, W., Di Valentino, E., Pan, S., & van de Bruck, C. 2025, <https://arxiv.org/abs/2507.11432>
- Leistedt, B., Peiris, H. V., & Verde, L. 2014, *Phys. Rev. Lett.*, 113, 041301, doi: [10.1103/PhysRevLett.113.041301](https://doi.org/10.1103/PhysRevLett.113.041301)

- Lewis, A. 2013, Phys. Rev. D, 87, 103529, doi: [10.1103/PhysRevD.87.103529](https://doi.org/10.1103/PhysRevD.87.103529)
- . 2019. <https://arxiv.org/abs/1910.13970>
- Lewis, A., & Bridle, S. 2002, Phys. Rev. D, 66, 103511, doi: [10.1103/PhysRevD.66.103511](https://doi.org/10.1103/PhysRevD.66.103511)
- Li, C., Wang, J., Zhang, D., Saridakis, E. N., & Cai, Y.-F. 2025a. <https://arxiv.org/abs/2504.07791>
- Li, J.-X., & Wang, S. 2025. <https://arxiv.org/abs/2506.22953>
- Li, T.-N., Du, G.-H., Li, Y.-H., et al. 2025b. <https://arxiv.org/abs/2501.07361>
- Li, T.-N., Du, G.-H., Wu, P.-J., et al. 2025c. <https://arxiv.org/abs/2507.13811>
- Li, T.-N., Li, Y.-H., Du, G.-H., et al. 2025d, Eur. Phys. J. C, 85, 608, doi: [10.1140/epjc/s10052-025-14279-7](https://doi.org/10.1140/epjc/s10052-025-14279-7)
- Li, T.-N., Wu, P.-J., Du, G.-H., et al. 2024, Astrophys. J., 976, 1, doi: [10.3847/1538-4357/ad87f0](https://doi.org/10.3847/1538-4357/ad87f0)
- Li, T.-N., Zhang, Y.-M., Yao, Y.-H., et al. 2025e. <https://arxiv.org/abs/2506.09819>
- Li, Y.-H., & Zhang, X. 2025. <https://arxiv.org/abs/2506.18477>
- Linder, E. V. 2003, Phys. Rev. Lett., 90, 091301, doi: [10.1103/PhysRevLett.90.091301](https://doi.org/10.1103/PhysRevLett.90.091301)
- Ling, J.-L., Du, G.-H., Li, T.-N., et al. 2025. <https://arxiv.org/abs/2505.22369>
- Liu, T., Li, X., Xu, T., Biesiada, M., & Wang, J. 2025. <https://arxiv.org/abs/2507.04265>
- Naredo-Tuero, D., Escudero, M., Fernández-Martínez, E., Marcano, X., & Poulin, V. 2024, Phys. Rev. D, 110, 123537, doi: [10.1103/PhysRevD.110.123537](https://doi.org/10.1103/PhysRevD.110.123537)
- Navas, S., et al. 2024, Phys. Rev. D, 110, 030001, doi: [10.1103/PhysRevD.110.030001](https://doi.org/10.1103/PhysRevD.110.030001)
- Nojiri, S., Odintsov, S. D., & Oikonomou, V. K. 2025. <https://arxiv.org/abs/2506.21010>
- Odintsov, S. D., Oikonomou, V. K., & Sharov, G. S. 2025. <https://arxiv.org/abs/2506.02245>
- Özülker, E., Di Valentino, E., & Giarè, W. 2025. <https://arxiv.org/abs/2506.19053>
- Pan, J., & Ye, G. 2025. <https://arxiv.org/abs/2503.19898>
- Pan, S., Paul, S., Saridakis, E. N., & Yang, W. 2025. <https://arxiv.org/abs/2504.00994>
- Pan, S., Seto, O., Takahashi, T., & Toda, Y. 2024, Phys. Rev. D, 110, 083524, doi: [10.1103/PhysRevD.110.083524](https://doi.org/10.1103/PhysRevD.110.083524)
- Pang, Y.-H., Zhang, X., & Huang, Q.-G. 2025, Sci. China Phys. Mech. Astron., 68, 280410, doi: [10.1007/s11433-025-2713-8](https://doi.org/10.1007/s11433-025-2713-8)
- Perlmutter, S., et al. 1999, Astrophys. J., 517, 565, doi: [10.1086/307221](https://doi.org/10.1086/307221)
- Qu, F. J., et al. 2024, Astrophys. J., 962, 112, doi: [10.3847/1538-4357/acfe06](https://doi.org/10.3847/1538-4357/acfe06)
- Riess, A. G., Filippenko, A. V., Peter., C., et al. 1998, Astron. J., 116, 1009, doi: [10.1086/300499](https://doi.org/10.1086/300499)
- Riess, A. G., Yuan, W.-L., Macri, L. M., et al. 2022, Astrophys. J. Lett., 934, L7, doi: [10.3847/2041-8213/ac5c5b](https://doi.org/10.3847/2041-8213/ac5c5b)
- Rosenberg, E., Gratton, S., & Efstathiou, G. 2022, Mon. Not. Roy. Astron. Soc., 517, 4620, doi: [10.1093/mnras/stac2744](https://doi.org/10.1093/mnras/stac2744)
- Roy Choudhury, S. 2025, Astrophys. J. Lett., 986, L31, doi: [10.3847/2041-8213/ade1cc](https://doi.org/10.3847/2041-8213/ade1cc)
- Roy Choudhury, S., & Choubey, S. 2018, JCAP, 09, 017, doi: [10.1088/1475-7516/2018/09/017](https://doi.org/10.1088/1475-7516/2018/09/017)
- Roy Choudhury, S., & Okumura, T. 2024, Astrophys. J. Lett., 976, L11, doi: [10.3847/2041-8213/ad8c26](https://doi.org/10.3847/2041-8213/ad8c26)
- Sabogal, M. A., Silva, E., Nunes, R. C., et al. 2024, Phys. Rev. D, 110, 123508, doi: [10.1103/PhysRevD.110.123508](https://doi.org/10.1103/PhysRevD.110.123508)
- Sahni, V., & Starobinsky, A. A. 2000, Int. J. Mod. Phys. D, 9, 373, doi: [10.1142/S0218271800000542](https://doi.org/10.1142/S0218271800000542)
- Silva, E., & Nunes, R. C. 2025. <https://arxiv.org/abs/2507.13989>
- Torrado, J., & Lewis, A. 2021, JCAP, 05, 057, doi: [10.1088/1475-7516/2021/05/057](https://doi.org/10.1088/1475-7516/2021/05/057)
- Vagnozzi, S. 2020, Phys. Rev. D, 102, 023518, doi: [10.1103/PhysRevD.102.023518](https://doi.org/10.1103/PhysRevD.102.023518)
- . 2023, Universe, 9, 393, doi: [10.3390/universe9090393](https://doi.org/10.3390/universe9090393)
- Vagnozzi, S., Dhawan, S., Gerbino, M., et al. 2018, Phys. Rev. D, 98, 083501, doi: [10.1103/PhysRevD.98.083501](https://doi.org/10.1103/PhysRevD.98.083501)
- Wang, H., & Piao, Y.-S. 2024. <https://arxiv.org/abs/2404.18579>
- . 2025. <https://arxiv.org/abs/2506.04306>
- Wu, P.-J. 2025. <https://arxiv.org/abs/2504.09054>
- Wu, P.-J., & Zhang, X. 2024. <https://arxiv.org/abs/2411.06356>
- Yang, W., Nunes, R. C., Pan, S., & Mota, D. F. 2017, Phys. Rev. D, 95, 103522, doi: [10.1103/PhysRevD.95.103522](https://doi.org/10.1103/PhysRevD.95.103522)
- Yang, W., Pan, S., Di Valentino, E., et al. 2025a, Phys. Rev. D, 111, 103509, doi: [10.1103/PhysRevD.111.103509](https://doi.org/10.1103/PhysRevD.111.103509)
- Yang, Y., Dai, X., & Wang, Y. 2025b, Phys. Rev. D, 111, 103534, doi: [10.1103/8ync-vrtz](https://doi.org/10.1103/8ync-vrtz)
- Yao, Y.-H., & Liu, J.-Q. 2025. <https://arxiv.org/abs/2507.00478>
- Yashiki, M. 2025. <https://arxiv.org/abs/2505.23382>
- Ye, G., Martinelli, M., Hu, B., & Silvestri, A. 2025, Phys. Rev. Lett., 134, 181002, doi: [10.1103/PhysRevLett.134.181002](https://doi.org/10.1103/PhysRevLett.134.181002)
- You, C., Wang, D., & Yang, T. 2025. <https://arxiv.org/abs/2504.00985>
- Zhang, J.-F., Li, Y.-H., & Zhang, X. 2015, Phys. Lett. B, 740, 359, doi: [10.1016/j.physletb.2014.12.012](https://doi.org/10.1016/j.physletb.2014.12.012)
- Zhang, X. 2016, Phys. Rev. D, 93, 083011, doi: [10.1103/PhysRevD.93.083011](https://doi.org/10.1103/PhysRevD.93.083011)
- . 2017, Sci. China Phys. Mech. Astron., 60, 060431, doi: [10.1007/s11433-017-9025-7](https://doi.org/10.1007/s11433-017-9025-7)